Hyperspectral remote sensing applications in mining impact analysis

C. Ehrler[a,*], C. Fischer[a], M. Bachmann[a]

[a] German Aerospace Center, German Remote Sensing Data Center, Dept. Land Surface, Oberfpaffenhofen, Germany –
(christoph.ehrler, c.fischer, martin.bachmann)@dlr.de

Abstract – Earth Observation (EO) data in combination with environmental data enables the extraction of important information for environmental management. There is a strong need in standardized and quality controlled data sets and reliable data analysis routines. Recent developments and established work flows at German Aerospace Center (DLR) include standardized pre-processing routines for geometric and atmospheric correction as well as deduced quality information parameter for different optical airborne and space borne sensor systems.

A comparison of various scene-optimized pre-processing options to the standardized procedure shows little benefits, contrary it worsens the results when efforts for high quality reference data are not undertaken. The effect of low quality topographic data in illumination correction is shown.

Based on a comprehensive hyperspectral data set an environmental assessment of acid mine drainage related pollution sources, pathways and pollution receptors is aspired. An overview of first analyses steps and current activities to resolve encountered problems is given.

Keywords: hyperspectral remote sensing, standardized pre-processing, topographic correction, mining impact analysis

1. INTRODUCTION

In recent years, the European Union's (EU) total material requirement has remained at a constantly high level. But in this time the weight of imports and their environmental impacts have considerably increased. As the EU is strongly interested in the establishment of measures based on material flow analysis, especially for imported mineral resources, the EC FP 7 project "*Earth Observation for Monitoring and Observing Environmental and Societal Impacts of Mineral Resources Exploration and Exploitation*" (EO-MINERS) will contribute to the development of those measures.

Based on the needs of industry, regulatory bodies and stakeholders, EO-MINERS starts with the identification of indicators and parameters to be taken into account in the assessment of the environmental, socio-economic and societal footprints of the extractive industry encompassing each stage of the operation, from exploration to exploitation and closure.

The aim is to bring into play EO-based methods and tools to facilitate and improve interaction between the mineral extractive industry and society in view of its sustainable development while improving its societal acceptability.

A strong component of EO-MINERS will consist in developing EO-based tools and methodologies to monitor, manage and contribute to reduce the environmental and societal footprint of extractive industry activities. The capabilities of integrated EO-based methods are to be demonstrated over three test sites located in heavily exploited areas:

1. Makmal gold deposit located in the Toguz-Toro region of the Jalal-Abad oblast of the Kyrgyz Republic, 630 km from Bishkek city in mountaineous terrain at 2350-2800 m above sea level. The main concerns lie in the necessity of a regular monitoring of water resources and soil on the heavy metals content in the impact zone of a tailing dump.

2. Witbank coalfields in Republic of South Africa lies 120 km from Johannesburg. This mining district covers a very large area and includes mines encompassing all stages of mining; from exploration through modern operating mines, mines undergoing closure and abandoned ownerless. The major impact of mining has been due to land degradation and water pollution. Old underground mine workings have collapsed, in some cases undergone spontaneous combustion.

3. The Sokolov lignite mining area is located in the North-West of the Bohemia province in Czech Republic, west of the town of Karlovy Vary. The area is largely affected by mining activities: open casts, closed mines and dump sites which are pollution sources with acid mine drainage (AMD) and related heavy metal contamination. In this region sulphide bearing materials, which can lead to the formation of acid mine drainage, include the coal and discarded material and some of the overburden materials used in the rehabilitation of open-pit operations.

For the Sokolov test site, which has been flown within two airborne hyperspectral flight surveys in 2009 and 2010, it is aspired to demonstrate the potential of hyperspectral data sets for environmental assessment and monitoring of pollution sources, pathways and pollution receptors.

Hyperspectral remote sensing is an extremely powerful technology to identify and map mineral occurrences at the topographic surface. Given the characteristic spectral signatures of the targeted minerals, their mixtures can be estimated and abundances can be calculated. Both are vital inputs for site-specific models to be developed during the project.

However, special care must be taken in the pre-processing steps. The goal is to generate standardized and quality controlled data sets facilitating multi-temporal analysis, robust analysis routines and derived product reliability statements.

2. HYPERSPECTRAL FLIGHT CAMPAIGN

Since 1995 the German Aerospace Center (DLR) is calibrating and operating airborne imaging spectrometers and is developing software tools for data processing and evaluation. Several national and international campaigns have been organised, co-ordinated and managed. The full system chain of sensor integration/adaptation to various aircraft, system calibration, campaign management, data processing, evaluation, archiving, and distribution is covered. This service called Optical Airborne

---

* Corresponding author.

Remote Sensing (OpAiRS) has been ISO certified (ISO 9001:2000) in November 2007 (Holzwarth et al., 2009).

In the course of the HyEurope2010 campaign the Sokolov test site was covered by seven flight lines at 6600 feet above ground level on 21 August 2010. Operating the HyVista Corporation's HyMap airborne hyperspectral scanner the datasets cover the spectral range 400 nm to 2500 nm with 126 bands at 4 meter ground resolution at nadir. Concurrent field spectrometer measurements and sampling on the ground provide data for validation and thematic analysis.
Both integrate into a comprehensive reference database comprising of reflectance measurements, chemical lab analyses, description of the stratigraphy and documentations over the last three years. Additionally hyperspectral image data of a HyMap campaign flown in summer 2009 with similar parameters exist.

3. PRE-PROCESSING

Dealing with data from different recording times, recording sensors and recording methods it is inevitable to define a common standardized way of pre-processing and quality control. Not before this the data can be evaluated in terms of pertinence and can serve as common data pool for all project activities.

3.1 OpAiRS routine pre-processing
Field spectra were collected with two ASD FieldSpec 3 instruments by the ground teams according to a protocol. The sampling pattern for each target area were blocks of target measurements in a regularly spaced grid bracketed by multiple white references at the beginning and the end. Several measurement blocks were taken for each target to adequately map its spectral variability.
The multiple white reference spectra enabled to check for changes in illumination and to exclude unreliable spectra. Apparent outliers were excluded and a mean spectrum, corrected for detector jumps and spectralon characteristics, was calculated for each target area.

The Sokolov 2010 HyMap data have been processed according to the OpAiRS certified standard processing chain for flat terrain. The Level 0 to Level 1 processing transforms the raw sensor output to digital numbers (DN) proportional to incoming radiance ($L_{at-sensor}$) taking internal sensor and detector characteristics into account. A HyVista system correction software is used. During the Level 1 to Level 2 processing DN are converted to $L_{at-sensor}$ according to Formula 1 where offset (c_0) and gain (c_1) are calibration coefficients.

$$L_{at-sensor} = c_0 + c_1 \cdot DN \qquad (1)$$

Both calibration coefficients are determined in a DLR operated laboratory called Calibration Home Base (Gege et al., 2009) on a vibration damped large optical bench. The implemented inflight calibration procedure (Richter, 1997) corrects for slight changes in those coefficients introduced by mounting the sensor into the airplane.
The ATCOR atmospheric and topographic correction module (Richter, 1998) normalises at-sensor radiance ($L_{at-sensor}$) to surface reflectance (ρ) taking atmospheric, topographic and viewing geometry effects into account. For the flat terrain processed Sokolov scenes no illumination or bi-directional reflectance distribution function (BRDF) corrections were performed.

In a last step the fully parametric orthorectification and geocoding module ORTHO (Müller et al., 2005) references the image data to a specified map projection.

Driven by the question how a site optimised pre-processing can improve the standard results the focus was set on inflight calibration and topographic modelling. Parameters influencing the atmospheric correction (e.g. water vapour content, horizontal visibility or aerosol type) can be confidently deducted from the multi-band HyMap imagery. Their variations in reasonable bounds show negligible effects at high visibility values of 60 – 80 km.

3.2 Test site optimised calibration coefficients
Several specific calibration coefficients were created based on calibration target field measurements during the HyMap overflight. A quality test based on the correlation coefficient of the target's regression between the image DN and the measured ground reflectance left two candidates: a 10,000 sqm bright orange kaolinitic quartz sand pile and a 2,500 sqm dark asphalt parking space.
When comparing image spectra and ground spectra it became obvious that both the asphalt and sand optimised calibration coefficients are inferior to the OpAiRS routine inflight calibration. Latter uses established and well monitored calibration targets imaged multiple times during every hyperspectral flight campaign and at best atmospheric and illumination conditions. The scene optimised calibration coefficients resulted in an artificial best-fit of the calibration target but introduced artefacts in the spectra of other surface materials (see Figure 1).
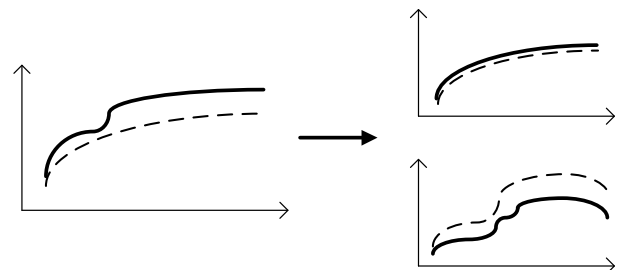

Figure 1. Adjacency influenced image spectrum (solid) to be forced by calibration coefficients onto pure ground target spectrum (dash) gives a nice match (right top) but introduces artefacts to other image spectra (right bottom).

3.3 Incorporation of topographic corrections
Several digital elevation models (DEM) were tested for inclusion of illumination and BRDF effect modelling in ATCOR. The hilly terrain in Sokolov with amplitude of few 100 meters does not introduce changes in atmospheric properties. Determinant is the slope and aspect of ground patches in relation to the sun, the local incident angle. Brightening of sun facing slopes and shadow casting are observable in many parts of the HyMap imagery and subject to correction efforts using ATCOR's topographic correction abilities.
Sokolov test site comprises of active mining areas thus changes in surface topography render historical or archived DEMs not suitable. For this reason the SRTM DEM, ASTER DEM, DLR internal global DEM and the DEM used in 2009 can not represent the actual topographic situation. A topographic correction using out-dated input will inevitably lead to unsatisfying results. Topographic features in the old DEM not

longer existing in reality will lead to ghost-brightening in the imagery, new features will not be corrected.

Figure 2 shows two additional DEMs which could be derived from optical stereo pairs of the Cartosat satellite sensor using an automated processor implemented at DLR (d'Angelo et al., 2009). Extensive cloud cover limited the usable archive data to two scenes. A cloud free pair of March 2009 could be used in order to estimate the accuracy of the satellite retrieved DEM compared to the 2009 DEM. The pair of September 2010 might be used to generate an up-to-date DEM but has cloud cover in the northern part of the scene.
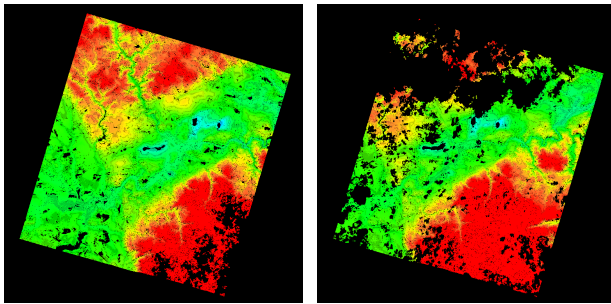

Figure 2. Cartosat-derived DEMs from 05.03.2009 (left) and 19.09.2010 (right). No correlation areas are coloured in black.

The difference images of the two Cartosat derived DEMs compared to the 2009 DEM (see Fugure 3) show the expected changes in the three mining areas. The statistics of a region of no change encompassing the whole southern overlap area yields a mean of -2.78 m and a standard deviation of 6.95 m for the Cartosat 2009 DEM, while the Cartosat 2010 DEM shows a mean of -2.23 m and a standard deviation of 7.05 m.
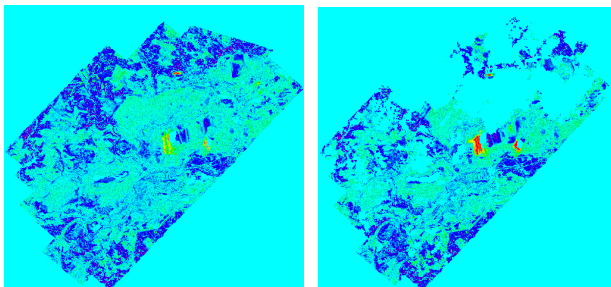

Figure 3. Coloured residual images for (left) Cartosat 2009 DEM minus 2009 DEM and (right) Cartosat 2010 DEM minus 2009 DEM. Cyan indicates "no deviation" or "no value", -45m purple … +45m red.

The residual of the Cartosat DEMs subtracted from each other yields a mean of 0.17 m and a standard deviation of 2.59 m for a region of no change encompassing the whole southern overlap area. This fits surprisingly well considering that both datasets were fully automated and independently derived from optical satellite data with no manual registration step.

The final Cartosat-derived 2010 DEM was created using the height information of the Cartosat 2010 DEM and filling its erroneous areas and gaps with data of the Cartosat 2009 DEM. Remaining gaps were filled by SRTM data. The difference to the 2009 DEM for the region of no change encompassing the whole southern overlap area yields a mean of -3.7 m and a standard deviation of 8.3 m. This is worse than either of the two individual Cartosat DEMs. The reason is the fact that no zero-filled gaps in the data exist after the merge which biased the statistical figures.

Using the merged DEM for topographic illumination correction the results were disappointing (see Figure 4). Strong brightening occurred at topographic transitions, e.g. from canopy to ground, at banquettes and at slopes in the mining sites. The effect could be reduced by enabling BRDF correction but was still very prominent. Apparently the quality of the merged DEM is not adequate and efforts have to be invested into DEM editing and co-registration. Simple smoothing filters will succeed in removing the overcorrection but eventually will fail in preserving the terraced shapes of the open-pit mine slopes. The reason is the similar spatial scale of the errors and the topographic features making it hard to differentiate between.

Figure 4. Effect of DEM errors on illumination correction. At-sensor radiance image (top left) with shadows. Overcorrection plus artefacts in surface reflectance image (top right) caused by DEM errors in slopes of mining area (bottom).

4. FIRST ANALYSES

Automated endmember extraction algorithms search for extreme points in the n-dimensional feature space of hyperspectral data. Thus they generally reported the most extreme image spectra including noise, artefacts, sun glint, coal fires and other hot surfaces, saturated pixels, artificial materials, etc. There was the tendency that subtle endmember spectra are left out. Therefore quality control and data normalization plus filtering steps needed to be implemented to exclude the disturbing data.
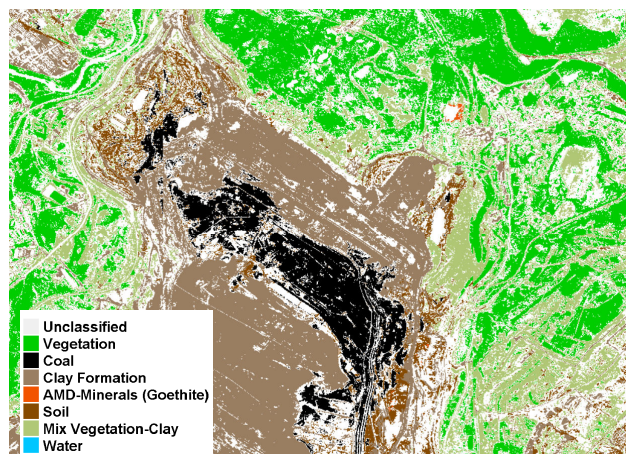

Figure 5. SAM classification image of lignite mining area.

A Spectral Angle Mapper (SAM) classification (see Figure 5) using mean spectra of manually defined training areas worked well but leaves space for improvements. Especially water bodies, dump materials and different clays were not satisfactory mapped.

The spectrally flat signature of coal with no absorption features as well as the unique water spectrum with no signature in the NIR to SWIR region makes them a "perfect" endmember for the spectral unmixing algorithms to mathematically optimize the result. Both can be used to adjust the albedo without introducing material-characteristic absorption features. Using an unconstrained linear spectral unmixing approach this resulted in considerable water and coal abundances in shadow pixels or pixels with materials not represented by the selected endmembers.

5. CONCLUSIONS & OUTLOOK

One of the major aim of EO-MINERS being to define tools opposable during discussions between the parties involved in a mining project life, a particular attention is paid to the definition and application of protocols and standards to EO data and added value products that guarantee the quality and objectivity of the data and products.
Here comes into play a fully integrated pre-processing chain as exists for airborne hyperspectral sensors with the OpAiRS service. For satellite imagery no such chain exists yet. However, lessons learned from airborne data can be adapted to satellite data and the atmospheric correction of satellite imagery can be readily accomplished by a specialised ATCOR module.

It could be shown that calibration and atmospheric correction of the airborne hyperspectral imagery can be satisfactory solved following the OpAiRS routine processing. Contrary conclusions must be drawn for the correction of illumination effects from topographic features. The lack of a high quality and accurately co-registered DEM leads to strong overcorrection in reflectance values. The merger of data from different quality and resolution levels imposes a challenge for the highly sensitive illumination correction. Solutions might be automated DEM-to-image registration, concurrent airborne laser scanning or sophisticated DEM editing using filters taking the topography into account.

Quality indicators for airborne and satellite imagery will be developed in the course of the project. Their application and accumulation during product generation will greatly benefit the ability of the user to judge quality, reliability and adequacy of the data.

The data analysis so far shows the need for advanced techniques to retrieve spectral endmembers, to perform spectral unmixing and to map mineral occurrences with finer differentiation. The endmember retrieval will benefit from laboratory spectra measurements of collected soil samples and the currently investigated capabilities of spatial-spectral endmember extraction (Rogget et al., 2007). Latter operates on subsets of the image data and employs singular value decomposition to retrieve also subtle endmembers which would be lost between the high spectral contrast endmembers of the whole image.
Spectral unmixing is believed to be improved by applying various constrained unmixing approaches and by a better understanding of mixtures of coal, clay and AMD minerals obtained from laboratory experiments.
A well suited endmember library and the knowledge of their mixture behaviour will finally lead to improved mapping results

which will be the input for further modelling tasks in EO-MINERS, e.g. pollution pathways, remediation success.
In general the advanced hyperspectral analysis results are intended to feed a set of indicators currently under development within the EO-MINERS project. They will contribute making available reliable and objective information about ecosystems, populations and societies affected by mining operations and serve as a basis for a sound trialogue between industrialists, governmental organisations and stakeholders.

REFERENCES

d'Angelo, P., Schwind, P., Krauss, T., Barner, F. and Reinartz, P., 2009. Automated DSM based Georeferencing of CARTOSAT-1 Stereo Scenes. In: ISPRS Hannover Workshop 2009 – High-Resolution Earth Imaging for Geospatial Information.

Gege, P., Fries, J., Haschberger, P., Schötz, P., Schwarzer, H., Strobl, P., Suhr, B., Ulbrich, G., Vreeling, W.J., 2009. Calibration facility for airborne imaging spectrometers. ISPRS Journal of Photogrammetry & Remote Sensing 64: 387-397.

Holzwarth, S., Weide, S., Bachmann, M., Gege, P., Müller, A., 2009. OpAiRS - Optical Airborne Remote Sensing and Calibration Facility. In 6th EARSeL SIG IS Workshop, Tel Aviv, Israel.

Müller, R., Holzwarth, S., Habermeyer, M., Müller, A., 2005. Ortho Image Production within an Automatic Processing Chain for hyperspectral Airborne Scanner ARES. EARSeL Workshop 3D-Remote Sensing, 3D RS Workshop, Porto, Portugal.

Richter, R., 1998. Correction of satellite imagery over mountainous terrain. Applied Optics 37(18).

Richter, R., 1997. On the inflight absolute calibration of high spatial resolution spaceborne sensors using small ground targets. Int. J. Remote Sensing 18: 2827-2833.

Rogge, D.M., Rivard, B., Zhang, J., Sanchez, A., Harris, J., Feng, J., 2007. Integration of spatial-spectral information for the improved extraction of endmembers. Remote Sensing of Environment 110(3): 287-303.